

# Analysis of Sensitivity for Low-Pass Multilayer Optical Filters

A.Massaro, L.Pierantoni, *Member IEEE*, C.Ciandrini, T.Rozzi, *Fellow IEEE*

Dipartimento di Elettromagnetismo e Bioingegneria, Università Politecnica delle Marche, via Brecce Bianche 12, I-60131, Ancona, Italy. e-mail: [MassaroAle@libero.it](mailto:MassaroAle@libero.it), [luca.pierantoni@univpm.it](mailto:luca.pierantoni@univpm.it), [C.Ciandrini@vodafone.it](mailto:C.Ciandrini@vodafone.it).

**Abstract** — Integrated optical and millimetric circuits produced by standard thin film-based technology suffer from manufacturing imperfections resulting in degradation of the absorption/diffraction response. Deposition through rf-bias sputtering is of particular interest in order to design an optical multilayered (Si and SiO<sub>2</sub>) filter. Geometrical imperfections like roughness at layer boundaries however gradually increase with the number of deposited layers. The low-pass filter specifications present high sensitivity to the errors of the exact values of ideal thickness and of ideal refractive indices. In this contribution, we evaluate the sensitivity of the specifications with respect to deviation from the exact values of refractive indices and thicknesses.

## I. INTRODUCTION

In optical filtering applications it is very important to determine the exact fabrication conditions. We analyze a low-pass filter multilayered structure presenting both i) a high refractive index  $n_H$ ; ii) a low refractive index  $n_L$  (see Fig.2) as reported in [1]-[3]. Due to deviations in the fabrication process (deposition technique, Fig.1), the frequency characteristics can be significantly affected. It is possible to reduce the amplitude of roughness below 0.3 nm through the use of rf-bias sputtering [1], but for a high number of layers the last few layers may present problems, whereas it is known that low-pass multilayered (Si and SiO<sub>2</sub>) filters are very sensitive to the parameters of the layers (refractive index and layer thickness). The goal of the present contribution is the analysis of the actual response of a multilayer (see Fig.2) filter originally designed from a Chebyshev prototype polynomials in order to fulfill low-pass specifications (Fig.3); for simplicity of analysis, we assume that all the refractive indices are non-absorbing and that the electrical length  $\theta_i$  are equal. After this prototype analysis, we perform a 3D full-wave simulation by using the Transmission Line Matrix-Integral Equation (TLMIE) method [5-6], where we vary the refractive index and estimate the Q factor sensitivity.

## II. THEORY

The low-pass filter of Fig. 2 was designed according to Chebyshev prototype in order to yield the squared magnitude response of the form

$$|H(j\omega)|^2 = \frac{1}{1 + h^2 T_N^2(\omega / \omega_c)} \quad (1)$$

where  $T_N(x)$  is the Nth-order (number of layers) Chebyshev (Fig. 3) polynomial defined by

$$T_N(x) = \cos(N \cos^{-1}(x)) = \cosh(N \cosh^{-1}(x)) \quad (2)$$

$\omega_c$  is the cutoff angular frequency. The filter specifications for the magnitude response in the passband and in the stopband are respectively:

$$1 \geq |H(j\omega)| \geq 1 - \delta_1 \quad |\omega| \leq \omega_c \quad (3)$$

$$|H(j\omega)| \leq \delta_2 \quad |\omega| \geq \omega_r \quad (4)$$

The Chebyshev polynomials (2) can be generated recursively by:

$$T_{N+1}(x) = 2xT_N(x) - T_{N-1}(x) \quad (5)$$

Since  $T_N(x)=1$  for any N, the squared magnitude response at cutoff equals  $1/(1+h^2)$ , and  $h^2$  is thus determined from the passband ripple  $\delta_1$  as

$$h^2 = \frac{1}{(1 - \delta_1)^2} - 1 = \frac{\left( \frac{n_H - n_{sub}}{n_{sub} n_L} \right)^2}{\left( \frac{n_H + n_{sub}}{n_{sub} n_L} \right)^2} \quad (6)$$

where the ripple factor has been established [4] for the ideally terminated multilayer. The required value of N for given stopband specifications is obtained from (1)-(4) as:

$$N = \left( \cosh \left( \sqrt{\frac{1 - \delta_2^2}{\delta_2^2 h^2}} \right) \right)^{-1} / \left( \cosh \left( \frac{\omega_r}{\omega_c} \right) \right)^{-1} \quad (7)$$

We observe that the number of the layers depends on the exact values of the refractive indices of the multilayer, so it is very important for the sputtering system to define the exact deposition condition [1] (oxygen-flow rate, temperature of substrate, total gas flow-rate, total gas pressure). In Fig.6 we show the variation of N: (a) for a substrate with a refractive index near the value of Si, (b) for a layer with a refractive index near the value  $n_L$  (SiO<sub>2</sub>). In the sensitivity of the number of layers we assume equal optical lengths:  $n_H t_H = n_L t_L$ , where  $t_H$  is the thickness

of the layer with a high refractive index, and  $t_L$  the thickness of the layer with a low refractive index. In Fig.5 we report the variation of the order  $N$  with  $t_L$  by varying the thickness of  $t_H$  of 1nm and 0.4 nm, in accordance with the roughness of the rf-sputtering technique. By fixing  $t_L$  more layers are necessary in order to satisfy the same specifications, in the case of variation of the thickness  $t_H$ . Hence, it is now possible first i) to evaluate the number of layers  $N$ , for a given specification, and then ii) the exact number  $N$  considering the roughness error. In Fig.7 we report the shift of the Chebyshev poles for a variation of  $t_H$  of 1 nm; it is seen that when the thickness  $t_H$  increases up to 226 nm, the minimum number of layers that can satisfy the specifications increases from  $N=7$  to  $N=8$ .

It is also possible to analyze the effect of the sensitivity by utilizing the ray model[5]: For a multilayer of homogeneous layers of alternately low and high refractive indices  $n_3$  and  $n_2$  and of thickness  $h_3$  and  $h_2$ , placed between two homogeneous media of refractive indices  $n_0$  and  $n_{sub}$ , if we assume  $\mu=1$  and set (TE analysis)

$$\beta_2 = \frac{2\pi}{\lambda} n_H d_H \cos \theta_H, \beta_3 = \frac{2\pi}{\lambda} n_L d_L \cos \theta_L, p_H = n_H \cos \theta_H, p_L = n_L \cos \theta_L, p_{sub,o} = \sqrt{\epsilon_{sub,o}} \mu \cdot \cos \theta_{sub,o} \quad (8)$$

where  $\theta$  is the ray-angle in the dielectric layers. The characteristic matrix of one period ( $t=d_H+d_L$ ) is

$$M_2(t) = \begin{bmatrix} \cos \beta_2 \cos \beta_3 - \frac{p_L}{p_H} \sin \beta_2 \sin \beta_3 & -\frac{i}{p_L} \cos \beta_2 \sin \beta_3 - \frac{i}{p_H} \sin \beta_2 \cos \beta_3 \\ -ip_H \sin \beta_2 \cos \beta_3 - ip_L \cos \beta_2 \sin \beta_3 & \cos \beta_2 \cos \beta_3 - \frac{p_H}{p_L} \sin \beta_2 \sin \beta_3 \end{bmatrix} \quad (9)$$

For  $2N$  films we have

$$M_{2N}(Nt) = \begin{bmatrix} M_{11} & M_{12} \\ M_{21} & M_{22} \end{bmatrix} \quad (10)$$

where

$$\begin{aligned} M_{11} &= \left( \cos \beta_2 \cos \beta_3 - \frac{p_L}{p_H} \sin \beta_2 \sin \beta_3 \right) u_{N-1}(a) - u_{N-2}(a) \\ M_{12} &= -i \left( \frac{1}{p_L} \cos \beta_2 \cos \beta_3 + \frac{1}{p_H} \sin \beta_2 \cos \beta_3 \right) u_{N-1}(a) \\ M_{21} &= -i \left( p_H \sin \beta_2 \cos \beta_3 + p_L \cos \beta_2 \sin \beta_3 \right) u_{N-1}(a) \\ M_{22} &= \left( \cos \beta_2 \cos \beta_3 - \frac{p_H}{p_L} \sin \beta_2 \sin \beta_3 \right) u_{N-1}(a) - u_{N-2}(a) \\ a &= \cos \beta_2 \cos \beta_3 - \frac{1}{2} \left( \frac{p_H}{p_L} + \frac{p_L}{p_H} \right) \sin \beta_2 \sin \beta_3 \end{aligned} \quad (11)$$

where  $U_N(x)$  are the Chebyshev Polynomials of the second kind. We observe that for the general case the reflectivity and the transmissivity are given by [5]

$$\Re = |r|^2 = \frac{\left( (M_{11} + M_{12} p_{sub}) p_o - (M_{21} + M_{22} p_{sub}) \right)^2}{\left( (M_{11} + M_{12} p_{sub}) p_o + (M_{21} + M_{22} p_{sub}) \right)^2} \quad (12)$$

$$\Im = \frac{p_{sub}}{p_o} \left| \frac{2 p_o}{(M_{11} + M_{12} p_{sub}) p_o + (M_{21} + M_{22} p_{sub})} \right|^2 \quad (13)$$

In Fig.8,9,10 is shown the sensitivity of the reflectivity for different values of refractive indices and thicknesses (normal incidence,  $n_o=n_{sub}=1$ ).

### III. TLMIE RESULTS

In the TLMIE method the physical *structure* is enclosed in a imaginary (rectangular) “box”, whose sides are the boundaries for the TLM-region (inside) and for the homogeneous regions (free-space/bulk region), [7]. This naturally leads to define the cavity-domain for the calculation of the Q-factor as the aforementioned “box”. We have:

$$Q = \frac{\omega_0 U}{W_L} \quad (14)$$

where  $\omega_0$  is the work angular frequency,  $U$  is the energy stored in the multilayered structure integrated on a period, and  $W_L$  is the dissipated power given by Poynting vector  $P_y(x,y,z;t)=E_z H_x - E_x H_z$ .

We observe that the Poynting vector is taken by starting from a reference plane (Fig.4), and in this case, in order to evaluate the Q factor for each frequency, we use a sinusoidal excitations of angular frequency  $\omega_0$ . The stored energy is evaluated by integrating the density ( $E_x^2 + E_z^2$ ) in the period of excitation and by using the Boundary Oriented Field-Mapping (BOFM) [6] approach. In Fig.11 we report the variation of Q factor and power losses in the case of a seven ( $S_i$  and  $S_iO_2$ ) layer low-pass filter; it is clear that in the transition band (middle region) the Q factor shows high sensitivity with respect to the refractive index (as shown in Fig.6).

### IV. CONCLUSION

In this contribution we deal with a real problems widely present in the realization of thin film layer optical filters: i) the effect of roughness at layer boundaries, ii) deviations from the exact values of the refractive indices and thickness, showing how these affect the realization of optical ( $Si$  and  $SiO_2$ ) filters. By using the accurate full-wave TLMIE method we investigate the behaviour Q factor as a function of optical parameters.

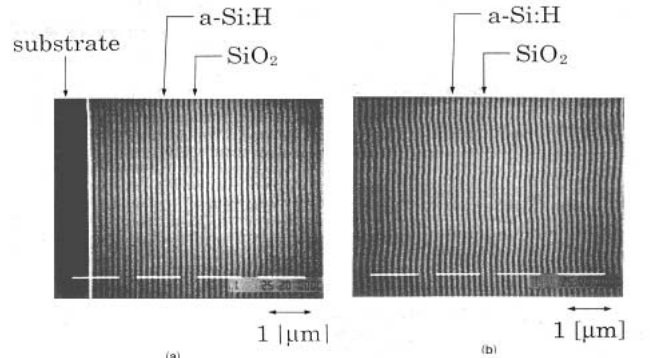


Fig. 1. Cross-sectional photographs in the vicinity of (a) the substrate and (b) the top surface.

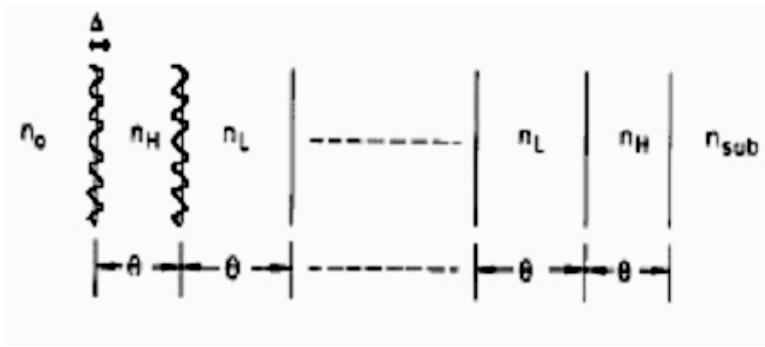


Fig. 2. Schematic representation of a low-pass multilayer filter with roughness of amplitude  $\Delta$  and  $n_0=1$  (air).

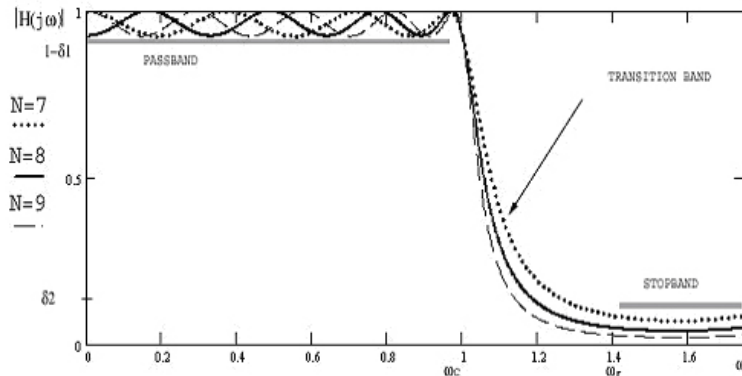


Fig.3. Classical low-pass filter specifications for the magnitude response and Type-I Chebyshev magnitude response of order N.

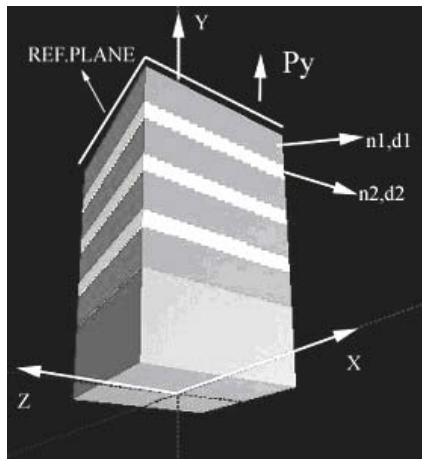


Fig.4. TLMIE simulated optical low pass filter.

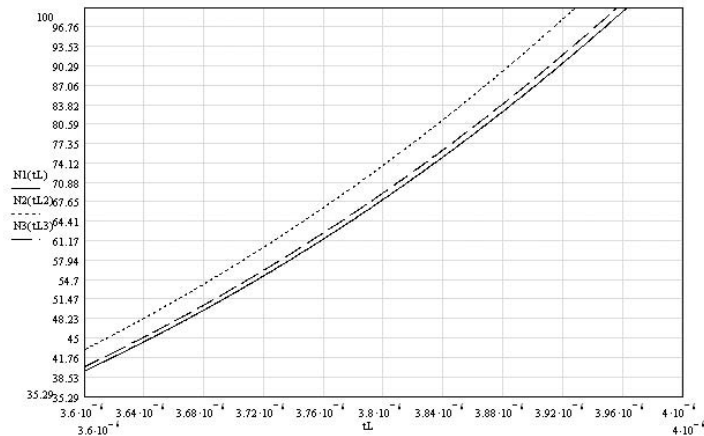


Fig.5. Variation of number of layers with the thickness  $t_L$  for  $\lambda_C=1.55 \mu\text{m}$ ,  $\lambda_r=0.09 \mu\text{m}$ ,  $n_{\text{sub}}=3.3$ ,  $n_L=1.45$ ,  $\delta_2=0.15$  ( $N_1$  for  $t_H=240 \text{ nm}$ ,  $N_2$  for  $t_H=230 \text{ nm}$ , and  $N_3$  for  $t_H=239.6 \text{ nm}$ ).

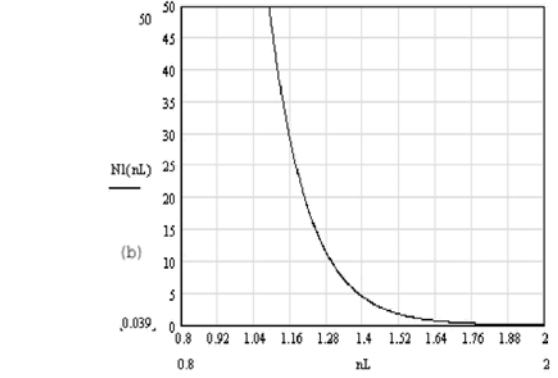
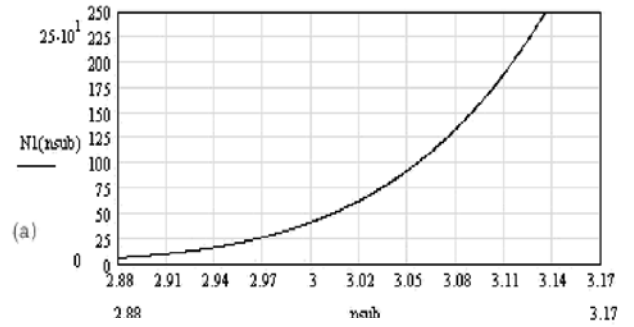


Fig.6. Variation of number of layers  $N_1=N$  with  $n_{\text{sub}}$  (a) using  $\lambda_C=1.55 \mu\text{m}$ ,  $\lambda_r=0.08 \mu\text{m}$ ,  $n_H=3.24$ ,  $n_L=1.45$ ,  $\delta_2=0.20$ , with  $n_L$ ,  $\lambda_r=1.55 \mu\text{m}$ ,  $\lambda_r=0.009 \mu\text{m}$ ,  $n_H=3.45$ ,  $n_{\text{sub}}=1.45$ ,  $\delta_2=0.15$ .

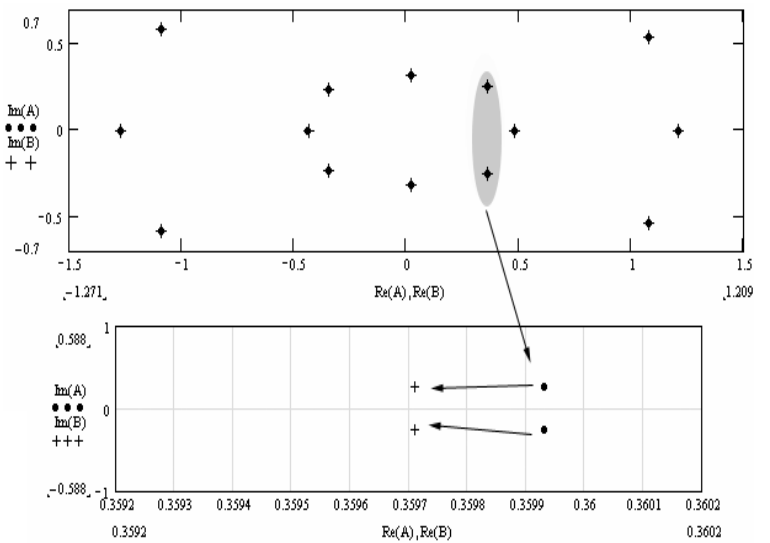


Fig.7: Variation of position of Chebyshev poles for a multilayer of 7 layers (sufficient to satisfy the specifications). A is the vector of poles for thickness  $t_L=100\text{nm}$ ,  $t_H=225\text{nm}$ ,  $\lambda_C=1.565 \mu\text{m}$ ,  $\lambda_r=0.09 \mu\text{m}$ ,  $n_{\text{sub}}=3$ ,  $n_H=3.24$ ,  $n_L=1.44$ ,  $\delta_2=0.15$ ,  $\delta_1=0.047$ ; B is the pole vector related to a variation of  $t_H$  of  $1\text{nm}$  ( $t_H=226 \text{ nm}$ ).

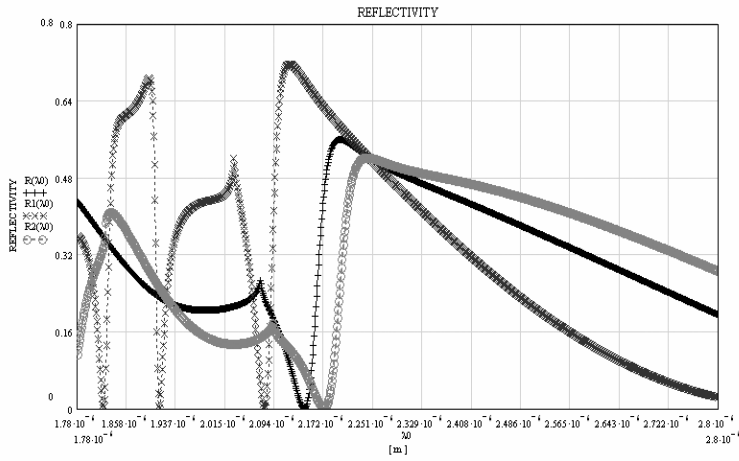


Fig. 8. Reflectivity using four  $S_i/S_iO_2$  layers with  $n_H=3.45$ ,  $t_H=0.4 \mu m$ ,  $t_L=0.26 \mu m$  (R for  $n_L=2$ , R1 for  $n_L=1.46$ , and R2 for  $n_L=2.2$ ).

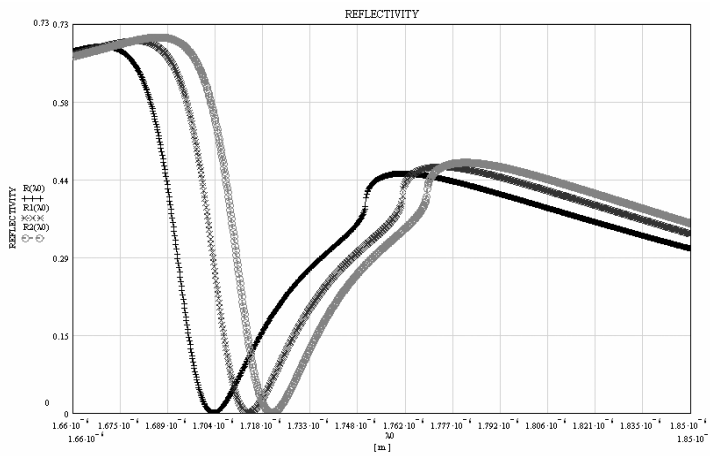


Fig. 9. Reflectivity using four  $S_i/S_iO_2$  layers with  $n_H=3.45$ ,  $n_L=2$ ,  $t_H=0.4 \mu m$ , (R for  $t_L=0.260 \mu m$ , R1 for  $t_L=0.266 \mu m$ , and R2 for  $t_L=0.27 \mu m$ ).

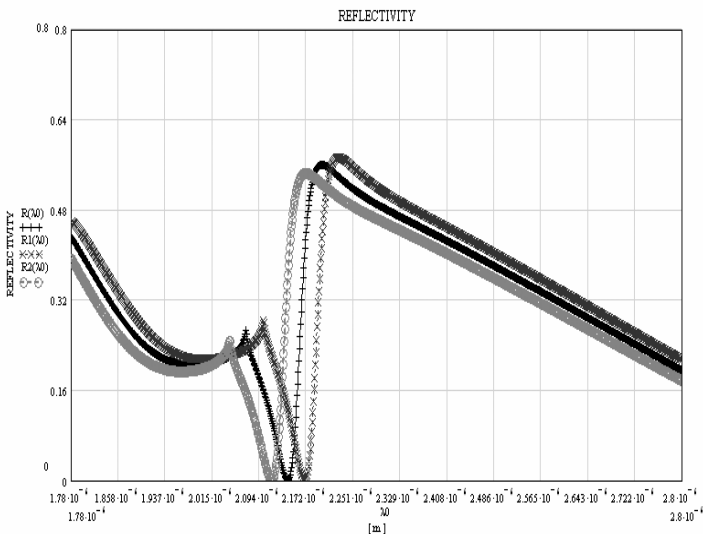


Fig. 10. Reflectivity using four  $S_i/S_iO_2$  layers with  $t_L=0.26 \mu m$ ,  $t_H=0.4 \mu m$ ,  $n_L=2$  (R for  $n_H=3.45$ , R1 for  $n_H=3.50$ , and R2 for  $n_H=3.40$ ).

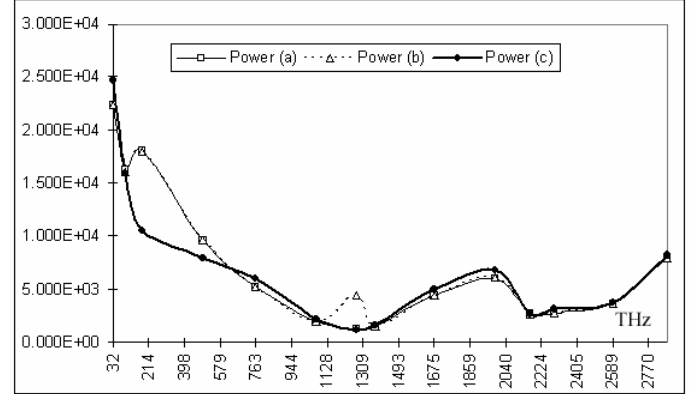
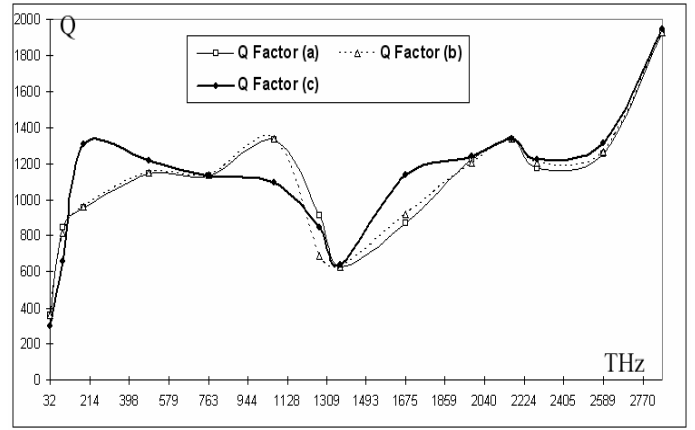


Fig. 11. TLMIE method- Q factor (above) and normalized power lost (below) of a simulated low-pass optical multilayered (7 layers) filter. a)  $t_L=100nm$ ,  $t_H=225nm$ ,  $n_{sub}=3$ ,  $n_H=3.24$ ,  $n_L=1.4$ , b)  $t_L=100nm$ ,  $t_H=225nm$ ,  $n_{sub}=3$ ,  $n_H=3.24$ ,  $n_L=1.44$ , c)  $t_L=100nm$ ,  $t_H=225nm$ ,  $n_{sub}=3.5$ ,  $n_H=3.34$ ,  $n_L=1.5$ .

## REFERENCES

- [1] T. Sato, T. Sasaki, K. Tsuchida, K. Shiraishi, S. Kawakami, "Scattering mechanism and reduction of insertion losses in a laminated polarization splitter", *Applied Optics*, Vol. 33 pp. 6925-6934, October 1994
- [2] Rhong-Chung Tyan, Pang-Chen Sun, Axel Scherer, and Yesha Yahu Fainman, "Polarizing beam splitter based on the anisotropic spectral reflectivity characteristic of form-birefringent multilayer gratings", *Optics Letters* vol.21, no.10/May 15 pp. 761-763.
- [3] A. Massaro, A. Di Donato, T. Rozzi, "Negative uniaxial optical behaviour of laminated polarization beam splitters" *GaAs2002 Conference*, Milan, pp.133.
- [4] T.C. Chen, "Optimised design of odd-order optical lowpass and highpass multilayer filters by method of coefficient matching", *IEE Proceedings*, Vol.135, No.2, April 1988.
- [5] M. Born and E. Wolf, *Principles of Optics*, 6th ed., Ed.: Cambridge University Press, 1980.
- [6] J. Rebel, "On the foundations of the Transmission Line Matrix Method", *Ph.D Thesis, Technische Univ. Muenchen*. December 1999.
- [7] L. Pierantoni, S. Lindenmeier and P. Russer, "A Combination of Integral Equation Method and FD/TLM Method for Efficient Solution of EMC Problems", *27th European Microwave Conf. (EuMC)*, Jerusalem, Israel, 8-12 September, 1997, pp. 93